

# Addressing uncertainty in fecal indicator bacteria dark inactivation rates

Andrew D. Gronewold<sup>a,\*</sup>, Luke Myers<sup>c</sup>, Jenise L. Swall<sup>b</sup>, Rachel T. Noble<sup>c</sup>

<sup>a</sup> Great Lakes Environmental Research Laboratory, NOAA, Ann Arbor, MI 48108, USA

<sup>b</sup> National Exposure Research Laboratory, USEPA, Research Triangle Park, NC 27711, USA

<sup>c</sup> Institute of Marine Sciences, UNC Chapel Hill, Morehead City, NC 28557, USA

---

## ARTICLE INFO

### Article history:

Received 22 February 2010

Received in revised form

6 August 2010

Accepted 13 August 2010

Available online xxx

---

### Keywords:

Water quality modeling

Fecal contamination

Bayesian

MPN

Decay rate

---

## ABSTRACT

Assessing the potential threat of fecal contamination in surface water often depends on model forecasts which assume that fecal indicator bacteria (FIB, a proxy for the concentration of pathogens found in fecal contamination from warm-blooded animals) are lost or removed from the water column at a certain rate (often referred to as an “inactivation” rate). In efforts to reduce human health risks in these water bodies, regulators enforce limits on easily-measured FIB concentrations, commonly reported as most probable number (MPN) and colony forming unit (CFU) values. Accurate assessment of the potential threat of fecal contamination, therefore, depends on propagating uncertainty surrounding “true” FIB concentrations into MPN and CFU values, inactivation rates, model forecasts, and management decisions. Here, we explore how empirical relationships between FIB inactivation rates and extrinsic factors might vary depending on how uncertainty in MPN values is expressed. Using water samples collected from the Neuse River Estuary (NRE) in eastern North Carolina, we compare *Escherichia coli* (EC) and *Enterococcus* (ENT) dark inactivation rates derived from two statistical models of first-order loss; a conventional model employing ordinary least-squares (OLS) regression with MPN values, and a novel Bayesian model utilizing the pattern of positive wells in an IDEXX Quanti-Tray<sup>®</sup>/2000 test. While our results suggest that EC dark inactivation rates tend to decrease as initial EC concentrations decrease and that ENT dark inactivation rates are relatively consistent across different ENT concentrations, we find these relationships depend upon model selection and model calibration procedures. We also find that our proposed Bayesian model provides a more defensible approach to quantifying uncertainty in microbiological assessments of water quality than the conventional MPN-based model, and that our proposed model represents a new strategy for developing robust relationships between environmental factors and FIB inactivation rates, and for reducing uncertainty in water resource management decisions.

© 2010 Published by Elsevier Ltd.

---

## 1. Introduction

Fecal contamination is a leading cause of surface water quality degradation in the United States (Mostaghimi et al., 2002; Noble et al., 2003a) and throughout the world (Ashbolt

et al., 1993; Ghinsberg et al., 1994). Roughly 20% of all total maximum daily load (TMDL) assessments approved by the United States Environmental Protection Agency (USEPA) since 1995, for example, address water bodies with unacceptably high fecal indicator bacteria (FIB) concentrations (a proxy for

## Nomenclature

|          |   |
|----------|---|
| Bi       | binomial distribution   |
| No       | normal distribution   |
| Po       | Poisson distribution  |
| St       | Student distribution  |
| $c, c_t$ | fecal indicator bacteria concentration at time $t$ (organisms per 100 ml)     |
| $c_0$    | fecal indicator bacteria concentration at time $t = 0$ (organisms per 100 ml) |
| $I$      | index of dilution series number   |
| $k, k'$  | first-order bacteria dark inactivation or loss rate (1/day)                   |
| $\ln$    | natural logarithm   |
| $N$      | number of wells in a dilution series  |
| $P$      | probability of a positive well in a dilution series                           |
| $t$      | time (days)   |

|     |  |
|-----|--|
| $v$ | volume of each well in a dilution series experiment (ml) |
| $y$ | number of positive wells in a dilution series            |

## Greek letters

|                       |   |
|-----------------------|---|
| $\epsilon, \epsilon'$ | model residual error terms  |
| $\lambda$             | mean and variance of the Poisson probability distribution             |
| $\mu$                 | location parameter in Student (St) probability distribution           |
| $\nu$                 | degrees of freedom in Student (St) probability distribution           |
| $\pi$                 | prior probability distribution  |
| $\sigma, \sigma'$     | standard deviation of $\epsilon, \epsilon'$ (ln organisms per 100 ml) |
| $\tau$                | scale parameter in Student (St) probability distribution              |

the measurement of fecal contamination-associated pathogens), the highest percentage of any pollutant category (for more on the TMDL program, see [National Research Council, 2001](#)).

Fecal contamination water quality assessments (within the context of the TMDL program and similar comprehensive water resource management programs) typically compare model-derived (or measured) FIB concentrations in a water body to a set of health risk-based numeric water quality standards ([Benham et al., 2006](#); [Gronewold et al., 2008](#)). Models supporting these assessments play a critical role by helping managers understand the potential threat waterborne pathogens pose to human health. This is true even for very simple models, such as those for calculating a geometric mean or 90th percentile, as outlined in the [Food and Drug Administration and Interstate Shellfish Sanitation Conference \(2005\)](#) proceedings and discussed further in [Boehm et al. \(2009\)](#). In addition, models provide the foundation for large-scale management decisions, such as whether or not to restrict access to a water body, or the extent to which pollutant loading levels must be reduced (through best management practices associated with the TMDL process, for example) so that receiving water bodies will comply with pertinent water quality standards.

Methodological variability associated with FIB concentration quantification methods is well-documented (see, for example [Griffin et al., 2001](#); [Noble et al., 2003b](#); [McBride, 2003](#); [Gronewold and Wolpert, 2008](#)) and, along with other extrinsic factors, can have a significant impact on a water quality-based management actions. Fully understanding and acknowledging these sources of variability represents an important step towards generating robust management decisions, such as the closing of a shellfish harvesting area or beach. More importantly, when uncertainty and variability are ignored or incorrectly quantified, they may lead to either overly-conservative management decisions, such as the closure of a beach or shellfish harvesting area when no true threat exists, or inadequate management interventions leading, perhaps, to human illness or the outbreak of disease.

Models that appropriately propagate uncertainty and variability from monitoring observations and environmental phenomena into water quality forecasts, therefore, could lead to more robust water resource management decisions, alleviate the need for intensive water quality sampling, and minimize detrimental impacts on human health. Models which fail to account for these potential sources of variability may lead to decisions with unfortunate human health consequences, and are therefore of limited practical use to water resource managers. We know of no studies, however, which perform a retrospective analysis of the strength of the relationship between model-based FIB concentration forecasts and actual human illness derived from contact with contaminated water. We believe this type of comparison would provide critical information towards improving model-based management decisions, and should be pursued in future research.

### 1.1. FIB inactivation rates and the first-order loss model

Models used to support FIB water quality assessments often include a parameter reflecting the effective rate of FIB loss over time due to natural die-off, settling, and other factors ([Auer and Niehaus, 1993](#); [Ferguson et al., 2003](#)). The magnitude of this rate, and its relationship to extrinsic factors, is typically assessed by calibrating a first-order loss model (see Section 2.4) using FIB concentration data collected in a controlled (e.g. laboratory) setting. Other model structures (second-order, for example) could be used, such as those discussed in [Borsuk and Stow \(2000\)](#) and [Huang and McBean \(2007\)](#). Here, we focus on the first-order loss model because it is commonly applied in FIB dark (i.e. in the absence of sunlight) inactivation rate studies, and because it provides an ideal template for us to explore alternative approaches to quantifying uncertainty.

In addition to [Auer and Niehaus \(1993\)](#) and [Ferguson et al. \(2003\)](#), [Sinton et al. \(1999\)](#) and [Noble et al. \(2004\)](#) suggest that FIB inactivation rates (also referred to as a “die-off” or “decay” rate) vary under different environmental conditions, including solar radiation, and water temperature (from here

forward, we refer to this rate as an “inactivation” rate). FIB inactivation rate variability in response to other factors, however, including initial FIB concentration and water column depth, is not as well-understood, and has been recommended as an area for future research. An implicit and more general objective of these studies, however, is to incorporate inactivation rates into comprehensive models with “real-world” data to forecast future FIB concentration dynamics over broad spatial (e.g. estuarine) and temporal (e.g. multiple years) scales. Despite this goal, documented inactivation rates (Bowie et al., 1985, for example) are rarely accompanied by an indication of the structure (e.g. first- or second-order) or performance (assessed, perhaps, through model confirmation) of the calibration model from which they were derived (Gronewold et al., 2009). This common oversight is particularly problematic because the calibration model may not be an appropriate representation of FIB concentration dynamics, leading to inaccurate estimates of inactivation rate magnitude and variability which could then propagate into undesired uncertainty and variability in “real-world” model applications.

### 1.2. FIB measurement uncertainty and variability

The two most common FIB concentration metrics are the most probable number (MPN) and the colony-forming unit (CFU). MPN and CFU values, when used to calibrate FIB inactivation rate models (such as the first-order loss model), contribute to variability in inactivation rate estimates and to discrepancies between observed and model-predicted concentration values (i.e. model error) in different ways due to unique intrinsic sources of bias and variability associated with MPN- and CFU-based testing procedures. Here, we focus on uncertainty and variability in MPN values alone. For more on addressing CFU value variability and incorporating it into FIB water quality models, see Gronewold et al. (2009).

There are a variety of MPN-based testing procedures, however the two most common for quantifying FIB concentrations are multiple-tube fermentation and chromogenic substrate tests. MPN values derived from these procedures are known to be positively biased (Garthright, 1993,1997) and have varying degrees of uncertainty depending on the design of the testing procedure, such as the number and volume of wells or tubes in a dilution series. Furthermore, each procedure can yield multiple sets of “raw” data (such as the pattern of positive wells in a dilution series) which, while leading to the same MPN value, might imply very different uncertainty bounds on the value of the “true” FIB concentration. Put differently, the “raw” data from an MPN-based experiment includes all of the information needed to quantify uncertainty and variability in the FIB concentration and to calculate an MPN value. Unfortunately, water quality scientists commonly report only MPN values, an approach which effectively discards valuable uncertainty and variability information contained in the “raw” data (Woodward, 1957; McBride, 2003).

Here, we explore ways to improve the estimation and representation of FIB inactivation rates for the purpose of increased accuracy in water quality management decisions. In the following section, we describe our approach to collecting and analyzing water quality data from an estuary in

eastern North Carolina. We then present a novel Bayesian model calibration procedure for quantifying FIB inactivation rates in estuarine waters, and explore the effect of potential extrinsic and intrinsic factors, including uncertainty in monitoring data, environmental conditions, and specific members of the FIB group being studied. We then compare the results of our proposed Bayesian model to those from a more conventional regression analysis, and conduct a model confirmation procedure (commonly referred to as a validation procedure) to assess model performance.

---

## 2. Methods

### 2.1. Monitoring plan and site description

Our study area is the Neuse River Estuary (NRE) near the city of New Bern in eastern North Carolina (NC). This area has been intensively studied and is selected for this study because it has historically high FIB concentrations relative to other sites in the NRE (Fries et al., 2006). The NRE is a typical Atlantic, lagoonal, largely wind-mixed estuary, and the water quality in the upper NRE is of economic and recreational importance to the surrounding area (Borsuk et al., 2001). Previous studies have indicated that NRE water quality suffers from anthropogenic FIB loading through stormwater runoff and upstream fecal contamination sources (Fries et al., 2006,2008).

### 2.2. Sample collection and inoculation

In order to assess dark inactivation rates of FIB populations at different concentrations, we inoculated environmental samples (i.e. collected *in situ*) from the NRE using inocula of influent from a nearby sewage treatment plant to achieve two different initial (i.e. post-inoculation) concentrations: 1) a “high” concentration (approximating a spill from a sewage treatment plant, for example), and 2) a “moderate” concentration approximating chronic stormwater runoff or a similar pollutant loading source.

Morehead City Wastewater Treatment Plant (MCWWTP) influent was collected in order to inoculate the environmental NRE samples. To enumerate FIB concentrations in the influent, duplicate 1.0 ml aliquots were diluted 100-fold along a four-point serial dilution. *Escherichia coli* (EC) and *Enterococcus* (ENT) concentrations (in organisms per 100 ml) were determined from a 100 ml diluted sample using appropriate IDEXX media and the IDEXX Quanti-Tray®/2000 kit (see Section 2.3 for details). The estimated MCWWTP influent FIB concentration was then used to calculate the appropriate volume of influent to inoculate water samples in an effort to achieve “target” final (post-inoculation) ENT concentrations of 3000 (“high”) and 300 (“moderate”) organisms per 100 ml.

Environmental grab samples (5 L each) were collected from both the surface and bottom water of the NRE study site on three dates (August 6, September 17, and October 16) in 2007. Three 1-L subsamples were poured from each sample, and placed in separate 1 L polycarbonate Nalgene bottles. Two of the three 1 L subsamples were inoculated with MCWWTP influent to achieve target concentrations. The third 1 L sample

from each set was not inoculated with MCW/WTP influent, and is referred to as the sample with a “baseline” FIB concentration.

After inoculation, each 1 L subsample was evenly split into two 500 ml subsamples which were then incubated in the dark at temperatures comparable to those in ambient NRE waters (22–28 °C), and individually shaken and uncapped to simulate environmental mixing and aeration every 8 h thereafter. Finally, water from the 500 ml subsamples was tested (as described in the following section) for EC and ENT concentrations (in organisms per 100 ml) at time intervals of roughly 0, 1, 2, and 3 days post-inoculation.

### 2.3. Sample enumeration

EC and ENT concentrations were quantified using the IDEXX Quanti-Tray®/2000 chromogenic substrate test (CST) kit with Colilert®-18 and Enterolert™ media. To ensure that FIB concentrations did not exceed the upper bound of the IDEXX Quanti-Tray®/2000 test (i.e. a test result with all positive wells in both dilution series), we followed manufacturer’s recommendations for implementing a 1:10 dilution factor by extracting duplicate 10.0 ml aliquots from each subsample and pipetting them into IDEXX 100 ml polycarbonate bottles containing 90 ml of deionized (DI) water and either Colilert®-18 and Enterolert™ media. Each bottle was shaken 25 times to ensure that the media was completely dissolved. The liquid was poured into an IDEXX Quanti-Tray/2000 tray, and the tray was sealed. Then, the trays containing the sample and the dissolved Colilert®-18 and Enterolert™ media were incubated at 35 °C for 18 h, and 41 °C for 24 h, respectively. “Raw” data, including the numbers of positive small and large wells for each set of trays, and the dilution factor (in this study, a dilution factor of 10 was used for all samples) was recorded according to manufacturer’s instructions. Finally, the number of positive large and small wells, along with the applicable dilution factor, were used to calculate the MPN (in organisms per 100 ml) for EC, ENT, and total coliforms. Total coliform results, however, were not used in this study.

### 2.4. Model calibration

FIB inactivation rates are often quantified by calibrating the following well-known first-order loss model (Fischer, 1979; Thomann and Mueller, 1987, pp. 145–147 and 56–59, respectively):

$$\frac{dc}{dt} = -kc, \quad c(t=0) = c(0) = c_0 \quad (1)$$

$$\ln c = \ln c_0 - k \times t$$

where  $c = c_t$  is the “true” (but unobserved) FIB concentration (in organisms per 100 ml) at time  $t$  (in days),  $c_0$  is the “true” FIB concentration at time  $t = 0$  (also in organisms per 100 ml), and  $k$  (in 1/days) is the first-order loss (or inactivation) rate. Here, we use  $k$  to represent FIB dark inactivation. In the following sections, we describe the two procedures used to calibrate this model.

#### 2.4.1. Conventional MPN-based approach

In the conventional MPN-based calibration approach, we assume (following common practice) that EC and ENT MPN values (in

organisms per 100 ml) are interchangeable with the “true” FIB concentration  $c$ , leading to the following calibration model:

$$\ln \text{MPN}_t = \ln c_0 - k \times t + \epsilon_t \quad (2)$$

$$\epsilon_t \sim \text{No}(0, \sigma) \quad (3)$$

where  $\text{MPN}_t$  represents the average MPN (based, in our study, on the average of two split samples) at each time step.

The model in equations (4) and (5) reflects the common assumption that discrepancies between the expected and observed values of the (logarithm of the) MPN can be described by a normally-distributed error term  $\epsilon$  (with mean 0 and standard deviation  $\sigma$ ). Although our calibration procedure allows different values of  $k$  and  $c_0$  for each experiment, we use subscripts in equations (4) and (5) to differentiate between times  $t$  after inoculation only (for clarity).

We estimate  $k$  and  $\sigma$  in equations (4) and (5) using a classical ordinary-least squares (OLS) regression procedure (for more on OLS regression, see Weisberg, 2005) in the `lm` package Chapter 4 (Chambers and Hastie, 1991: Chapter 4) in the statistical software program R (Ihaka and Gentleman, 1996).

#### 2.4.2. Proposed “raw” data-based approach

In our proposed “raw” data-based approach, we deliberately avoid calculating or using MPN values, and instead consider the pattern of positive wells from the IDEXX Quanti-Tray®/2000 test kit as data (hereafter referred to as “raw” data). In this approach, we calibrate the first-order loss model by assuming (following Hurley and Roscoe, 1983; McBride, 2003) that the number of positive wells in each dilution series of an IDEXX Quanti-Tray®/2000 test kit are independent binomial random variables,  $y_i \sim \text{Bi}(n_i, p_i)$ , where (in dilution series  $i$  from any given sample)  $y_i$  is the number of positive wells,  $n_i$  is the total number of wells,  $p_i = 1 - e^{-c v_i / 100}$  is the probability of a positive well,  $c$  (in organisms per 100 ml) is the “true” but unobserved FIB concentration, and  $v_i$  is the volume (in ml) of each well in dilution series  $i$ . For the IDEXX Quanti-Tray®/2000 kit,  $i \in \{1, 2\}$ ,  $n_1 = 49$ ,  $n_2 = 48$ ,  $v_1 = 1.86$  ml, and  $v_2 = 0.186$  ml. These assumptions, when combined with equation (1), lead to the following calibration model (for clarity, subscripts differentiate only between dilution series  $i$  and times  $t$  after inoculation):

$$y_{i,t} | n_i, p_{i,t} \sim \text{Bi}(n_i, p_{i,t}) \quad (4)$$

$$p_{i,t} = 1 - e^{-c_t v_i / 100} \quad (5)$$

$$\ln c_t = \ln c'_0 - k' \times t + \epsilon'_t \quad (6)$$

$$\epsilon'_t \sim \text{No}(0, \sigma') \quad (7)$$

where  $\epsilon'$  is a normally-distributed error term with mean 0 and standard deviation  $\sigma'$ .

The rationale for equations (6) through (9), and for distinguishing a “raw” data-based model from the conventional MPN-based model, can be explained, in part, through the graphical model in Fig. 1. This graphical model reflects the assumed relationship between the FIB concentration  $c$  in a sample at time  $t$ , the dark inactivation rate ( $k, k'$ ), the associated pattern of positive wells ( $y_1$  and  $y_2$ ) given  $c$ , and an MPN value. The variables and parameters included in our proposed

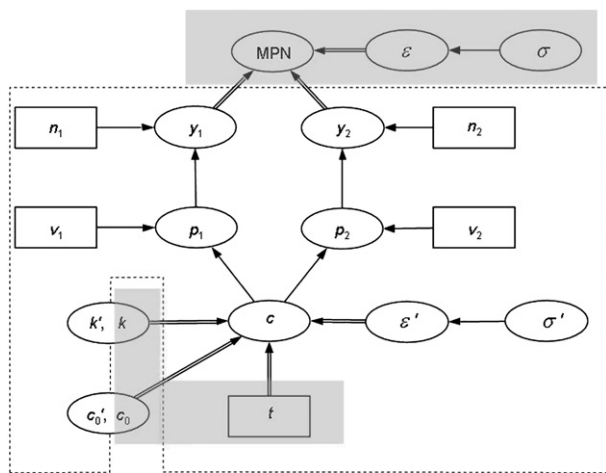


**Fig. 1 – Graphical representation of first-order FIB loss model and the IDEXX Quanti-Tray®/2000 procedure. Dashed lines bound variables and parameters (both ovals) and constants (rectangles) in our proposed “raw” data-based model equations (6)–(9), while the shaded regions include variables, parameters, and constants in the conventional MPN-based model equations (4) and (5). Single-lined arrows lead to stochastic (i.e. defined by a probability distribution) model variables and parameters, while double-lined arrows lead to deterministic model variables.**

“raw” data-based calibration model are bounded by dashed lines in Fig. 1, while those included in the conventional MPN-based calibration model are shaded. In particular, Fig. 1 indicates how our proposed “raw” data-based procedure infers the dark inactivation rate ( $k'$ ) by first quantifying uncertainty in the true but unobserved FIB concentration  $c$ . In contrast, the dark inactivation rate derived from the conventional MPN-based procedure ( $k$ ) is based on an assumption that the MPN and  $c$  are interchangeable.

We encode equations (4)–(7) within a Bayesian framework (for more on Bayesian statistics, see Berry, 1996; Bolstad, 2004), an approach which allows us to utilize all of the “raw” data from a serial dilution experiment and to express the number of positive wells in a dilution series as a binomial random variable (equations (4) and (5)). Encoding equations (6)–(9) in a Bayesian framework also allows us to infer the FIB dark inactivation rate ( $k'$ ) by combining *a priori* beliefs with empirical evidence using Bayes’ theorem (Bayes 1763). In this approach, *a priori* beliefs regarding potential values of  $k'$  are expressed through a prior probability distribution,  $\pi(k')$ , while values of  $k'$  supported by empirical evidence are expressed through a likelihood function. Bayes’ theorem combines these two sources of information into a posterior probability distribution.

Here, we specify an informative prior probability distribution for  $k'$  drawing from documented values in previous FIB inactivation rate studies (Bowie et al., 1985). Using these historic values as a guide to likely values of  $k'$ , we choose a Student (St) prior distribution,  $\pi(k') \sim \text{St}(\mu, \tau, \nu)$ , with location  $\mu = 0.15$ , scale  $\tau = 1$ , and degrees of freedom  $\nu = 3$ . The Student (St) distribution (Bernardo and Smith, 1994, pp. 122–123), particularly when compared to more common prior probability distributions, is ideal for our study because

it reflects the range of previously documented inactivation rates and accommodates potential values which might be supported by our analysis (including both very high and negative inactivation rates).

We estimate  $k'$  and  $\sigma'$  in equations (8) and (9) by simulating samples from their respective posterior distributions (for definitions, see Press, 2003; Bolstad 2004; Chapter 4 and Section 4.6, respectively) using Markov chain Monte Carlo (MCMC) procedures in the software program WinBUGS (Lunn et al., 2000). We ran each MCMC chain until it reached convergence, indicated by a potential scale reduction factor  $\hat{R} = 1.0$  (Gelman et al., 2004, pg. 297). Computer code for our Bayesian model is included in the appendix.

## 2.5. Model confirmation

We evaluate the predictive performance of the conventional MPN-based model and our proposed “raw” data-based model using a “leave-one-out” cross-confirmation procedure (for details, see Efron and Tibshirani, 1993, pps. 240–241). We recognize that while this procedure is commonly referred to as validation, we prefer the term confirmation, since validation implies an ascertainment of truth, and only applies when the model is compared to independent observations (Reckhow and Chapra, 1983).

To confirm the MPN-based model, we begin by using the “leave-one-out”-based parameter sets to predict MPN values at each time step. This approach is based on the common assumption that the MPN-based model, because it is calibrated using MPN values from the IDEXX Quanti-Tray®/2000 procedure, implicitly predicts MPN values (as opposed to FIB concentration values or CFU values). We then construct 95% prediction intervals (Weisberg, 2005) for each MPN value using the 0.025 and 0.975 quantiles of the predictive probability distribution implied by the model in equation (5). Finally, we calculate the fraction of observed MPN values within each interval.

We confirm our proposed “raw” data-based model by following the logic of equations (6)–(9). First, we use the “leave-one-out” parameter sets to simulate 10,000 samples from the FIB concentration ( $c$ ) probability distribution (equations (6) and (7)) at each time step  $t$ . We then simulate the pattern of positive wells ( $y_1, y_2, t$ ) from an IDEXX Quanti-Tray®/2000 procedure (equations (6) and (7)) for each simulated sample and calculate the MPN value following (Woodward, 1957; Hurley and Roscoe, 1983). Using the 10,000 simulated MPN values for each time  $t$  in each experiment we then construct a 95% MPN prediction set which, following Gronewold and Wolpert (2008), is defined as the set of highest probability MPN values for which the cumulative probability mass is at least 0.95. Finally, we calculate the fraction of observed MPN values which coincide with each discrete 95% prediction set.

## 3. Results

### 3.1. FIB concentration analysis and inactivation rate assessment

Our water quality analysis results indicate that inoculated samples corresponding to “high” and “moderate” EC and ENT

concentrations decrease at rates approximately represented by a log-linear model, although the rate of decrease appears greater for higher starting concentrations (first and fourth rows in Fig. 2). Dynamics for relatively low EC and ENT concentrations, however, are less clear, in part because the rate of change appears to fluctuate across different sampling dates, and in part because the uncertainty in monitoring data is more pronounced at low concentrations (third and sixth rows in Fig. 2). We also note that the native bacteria organisms

in the baseline sample may be from a different population than those in the “high” and “moderate” concentration samples, and that this difference may limit our comparison between the corresponding inactivation rates.

Our inactivation rate assessment (i.e. model calibration) results (Fig. 3) indicate that EC dark inactivation rates (left two panels) decrease as initial EC concentration decreases, and this relationship is consistent across sample depth and between the two model calibration procedures. In particular,

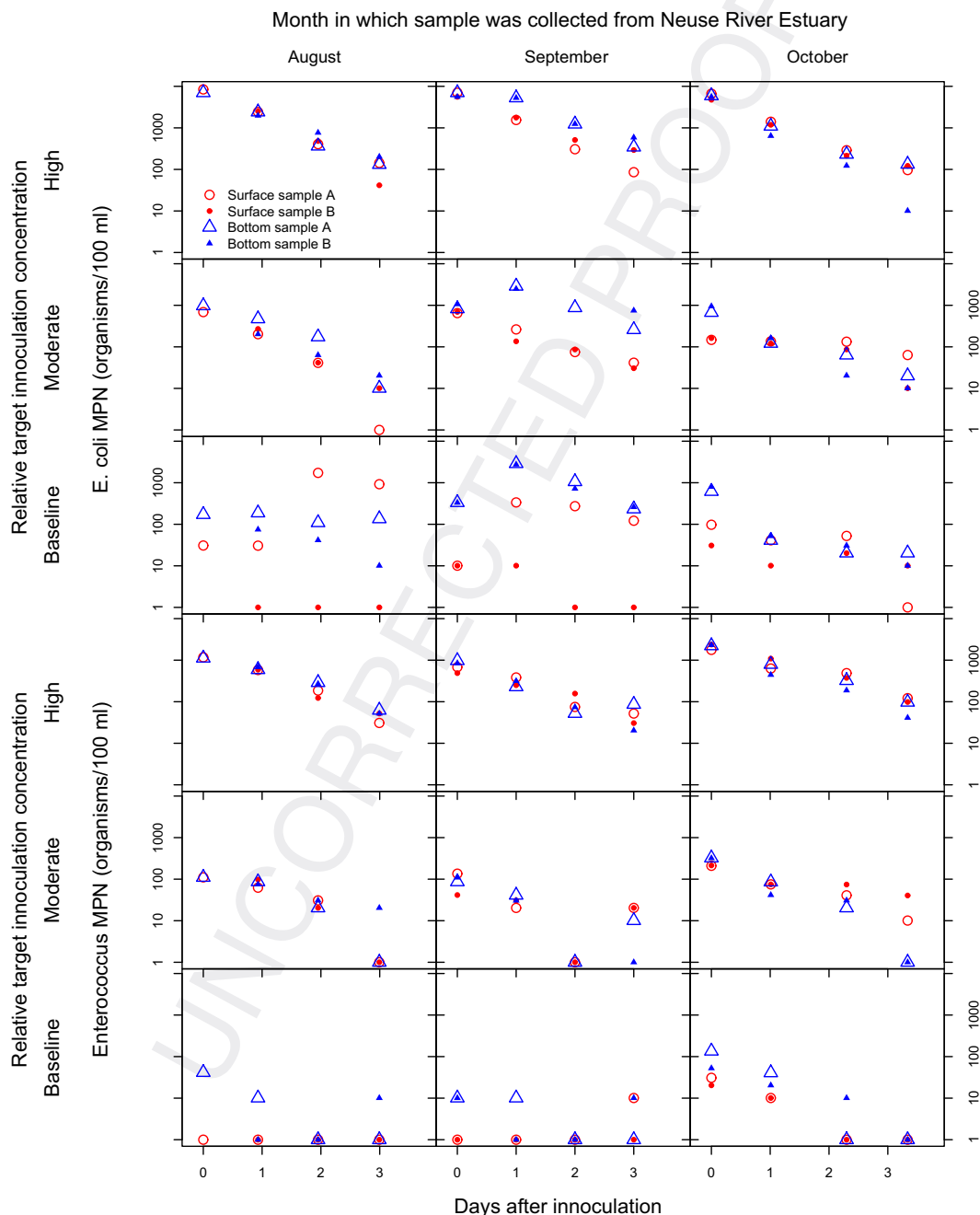


**Fig. 2 – EC (top 3 rows) and ENT (bottom 3 rows) MPN values (in organisms per 100 ml) at times  $t$  (days) after inoculation. Rows within each FIB type correspond to “high”, “moderate”, or “baseline” post-inoculation concentrations. Columns correspond to months when in situ samples were collected from the NRE. Samples collected from the surface are represented by red circles. Samples collected from the bottom are represented by blue triangles. Split samples are distinguished as sample A (hollow shapes) and sample B (filled shapes).**

our results indicate that EC dark inactivation rates are likely to be negative at concentrations at or below approximately 30–50 organisms per 100 ml (suggesting the potential for sustained populations or regrowth at low concentrations). Our results also indicate that the “raw” data-based model leads to slightly narrower credible interval estimates for EC dark inactivation rates (black horizontal lines) when compared to confidence intervals derived from the conventional MPN-based model (grey horizontal lines).

The relationship between ENT dark inactivation rates (right panels in Fig. 3) and initial concentration, depth, and model selection is not as clear. Most noticeably, our results indicate that the magnitude and uncertainty associated with ENT dark inactivation rate estimates depends on the model from which the estimate was derived. In particular, uncertainty in ENT dark inactivation rates derived from the MPN-based model (grey lines) is relatively consistent across all extrinsic factors, while the uncertainty in estimated ENT dark inactivation rates derived from our “raw” data-based model (black lines) increases as FIB concentration decreases. Furthermore, while our results do not indicate a significant overall trend in the magnitude of ENT dark inactivation rates relative to initial ENT

concentration, they do indicate that ENT dark inactivation rates derived from the conventional MPN-based model may be significantly lower at ENT concentrations close to 1 organism per 100 ml when compared to higher ENT concentrations.

Finally, our results indicate that the two calibration models lead to very different estimates of model residual standard deviation ( $\sigma$ ,  $\sigma'$ ) and that the magnitude of the difference depends on which FIB organism is studied (Fig. 4). For example, the residual standard deviation in the MPN-based model ranged between 0.72 and 1.1 when using EC data (grey lines in top panel, Fig. 4) and between 0.75 and 1.15 when using ENT data (grey lines in bottom panel, Fig. 4). The residual standard deviation in the “raw” data-based model, meanwhile, ranged between 0.6 and 0.96 when using EC data (black lines in top panel, Fig. 4) and between 0.12 and 0.35 using ENT data (black lines in bottom panel, Fig. 4).

### 3.2. Model confirmation

Model confirmation results for 20 representative EC samples are presented in Fig. 5, which compares EC MPN values (circles in Fig. 5 with duplicates, if analyzed, distinguished by color)

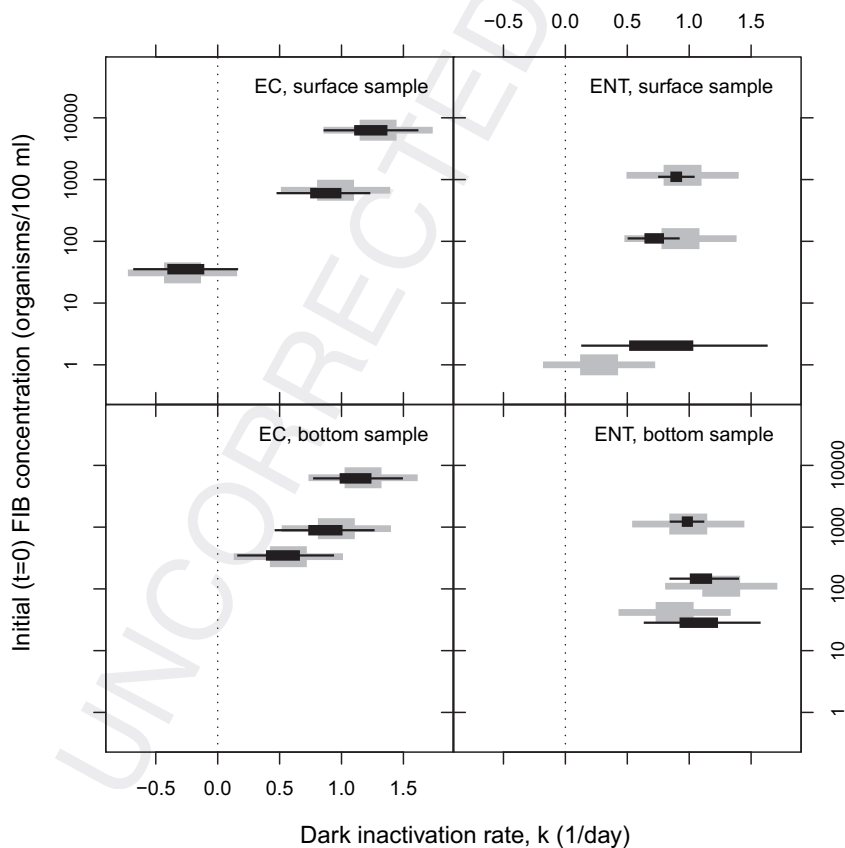


**Fig. 3 – Relationship between FIB dark inactivation rate estimates ( $k$ ) and measured (as opposed to “target”) initial FIB concentration for each combination of sample depth (surface or bottom) and FIB species (EC or ENT). Dark inactivation rate interval estimates (horizontal lines) were derived from experiments with either “high” (top black and grey lines in each panel), “moderate” (middle black and grey lines in each panel), or “baseline” (bottom black and grey lines in each panel) target post-inoculation concentrations. Black lines represent 95% (thin lines) and 50% (thick lines) credible intervals derived from our “raw” data-based model, while grey lines represent 95% and 50% confidence intervals derived from the conventional MPN-based model. The vertical dashed line at  $k = 0$  is included to help distinguish between positive and negative inactivation rates.**

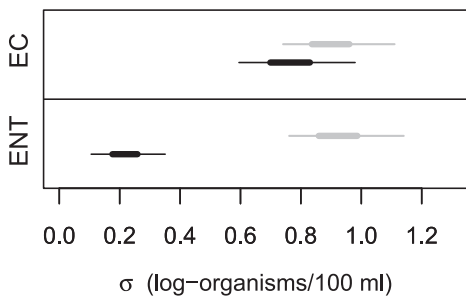


**Fig. 4 – 95% (thin lines) and 50% (thick lines) intervals for model residual standard deviation ( $\sigma$ ) from the “raw” data-based model (black lines) and the conventional MPN-based model (grey lines). Results are presented separately for models calibrated to EC data (top panel) and ENT data (bottom panel).**

with cross-confirmation 95% confidence intervals derived from the MPN-based model (left-hand panel) and 95% prediction sets derived from the “raw” data-based (i.e. Bayesian) model (right-hand panel). Sample 1, for example, which was not analyzed in duplicate, yielded an MPN value of 31 organisms per 100 ml (bottom blue dot in both panels of Fig. 5) which is within the 95% prediction intervals derived from the conventional MPN-based model, and coincides with an MPN

value in the 95% prediction set derived from the “raw” data-based model.

Of the 137 samples analyzed (72 samples, 65 analyzed in duplicate) for both EC and ENT concentration, 118 (86%) EC MPN values and 124 (91%) ENT MPN values were within 95% cross-confirmation prediction intervals derived from the conventional MPN-based model. Similarly, 125 (91%) EC MPN values and 121 (88%) ENT MPN values coincided with 95% prediction sets derived from our “raw” data-based model.

#### 4. Discussion

We have presented two approaches to calibrating a first-order FIB loss model to assess FIB dark inactivation rates, and have demonstrated that the magnitude and uncertainty of the assessed rates may vary depending on FIB species and initial FIB concentration, but that these relationships might be contingent upon how the inactivation rate model is calibrated and, consequently, how uncertainty is expressed in the estimated inactivation rate. Applicability of these findings beyond the scope of this study (to large-scale water quality model-based assessments, for example), however, depends not only on environmental conditions (such as sunlight intensity and salinity, among others) but also on the predictive performance of the calibration models from which they were derived (Gronewold

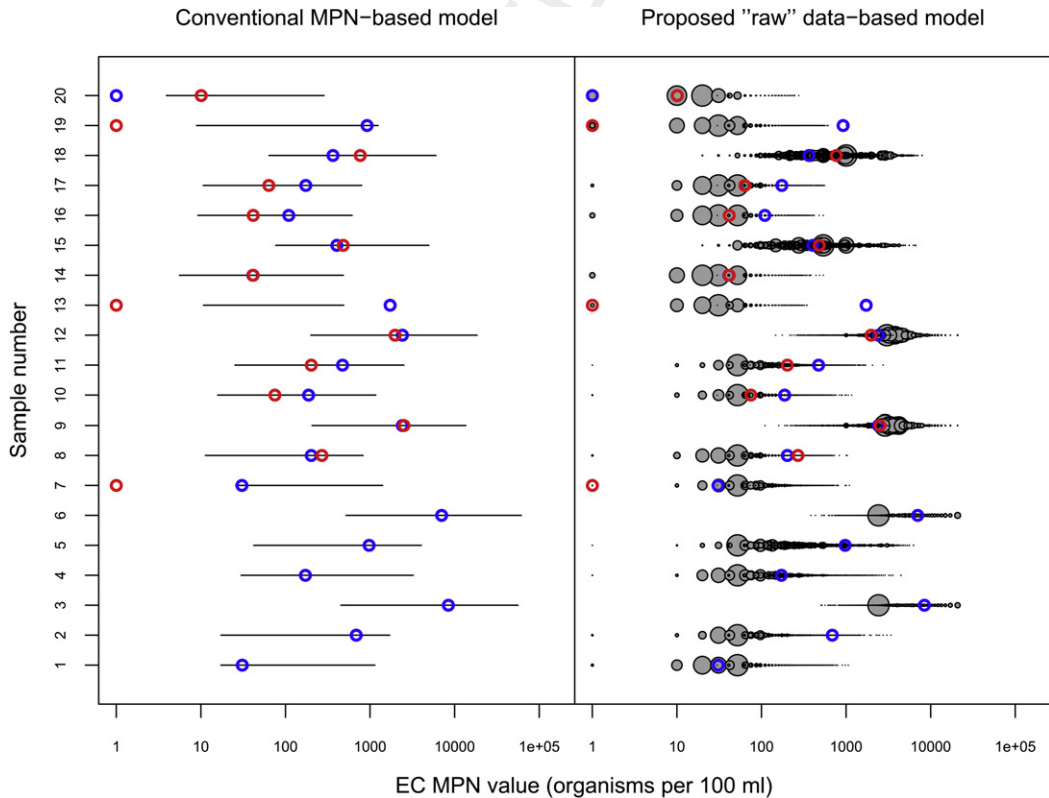


**Fig. 5 – Model confirmation results for 20 representative (of 72 total) EC analysis events, including 95% prediction intervals derived (via cross-confirmation) from the MPN-based model (horizontal black lines in left panel) and 95% prediction sets derived from the “raw” data-based model (grey circles in right panel). The diameter of the grey circles in the right panel is proportional to the probability mass of the corresponding MPN value Gronewold and Wolpert (2008). Observed MPN values are represented by red and blue circles (with duplicates distinguished by color). Samples 1–6 were not analyzed in duplicate.**

et al., 2009). Indeed, both model calibration procedures appear to lead to reasonable confirmation results (proposed 95% intervals and sets collectively include 86–91% of all MPN values), yet we suspect that the inability of these intervals to capture more of the variability in MPN values is strongly associated with how the MPN and “raw” data from a serial dilution analysis procedure are used (or not used) in model inference. Consequently, understanding how and why the MPN might contribute to poorer-than-expected model performance and, conversely, how the use of “raw” data might address those causes, has significant implications for both “real-world” (i.e. management action-based) and research-oriented applications.

To begin, we note that 95% prediction intervals derived from the conventional MPN-based model (left-hand panel in Fig. 5) are commonly assumed to reflect all sources of variability in MPN values, including those arising from FIB fate and transport, and through the MPN analysis procedure. The conventional MPN-based model, however, is often calibrated using *average* MPN values from two split samples (a practice we follow in this study). Thus, the 95% prediction intervals in the left-hand panel in Fig. 5 are, in fact, prediction intervals for the *average* MPN value, and the fact that a relatively high percentage (86–91%, depending on FIB species) of the *non-averaged* MPN values (i.e. blue and red circles in Fig. 5) are within these intervals indicates that the MPN-based model may lead to unnecessarily large prediction intervals and, potentially, to overly-conservative management decisions. In contrast, the “raw” data-based model did not utilize average values, and instead treated the pattern of positive wells from the serial dilution analysis as independent observations arising from a common FIB concentration, an approach which ultimately allows us to propagate uncertainty in the FIB concentration estimate into an estimated inactivation rate, a quantification of model error and, ultimately, into a model-based forecast of likely MPN values.

Another complication in the conventional MPN-based model is the absence of a protocol for reporting an MPN value when an IDEXX kit (or other serial dilution analysis test) yields no positive wells in either dilution series (i.e.  $y_1 = y_2 = 0$ ), yet we recognize this result is often reported as an MPN value  $\leq 1.0$  organism per 100 ml (i.e. the MPN value when only one well from only one dilution series is positive). Following Gronewold and Wolpert (2008), we argue that a result of all wells negative is best explained by a concentration of 0 organisms per 100 ml, though other values are possible, and the corresponding MPN values should be 0 organisms per 100 ml (for details, see Hurley and Roscoe, 1983; McBride, 2003). Of course, an MPN value of 0 organisms per 100 ml is incompatible with the conventional MPN-based model (equation (2)) because the logarithm of 0 is not finite. Furthermore, the range of feasible MPN values in this study is limited because the MPN probability distribution is intrinsically discrete, and because a 1:10 dilution factor was used in the study design, limiting the range of potential MPN values. Thus, while the discrete nature of the MPN probability distribution and the value assigned to an “all wells negative” result clearly impact our water quality analysis results and potential assessments derived from those results, neither is adequately reflected in the MPN-based model confidence intervals (left panel Fig. 5). For example, all of the MPN-based model intervals imply a continuous range of potential MPN values with the most likely values closest to the center of each interval. The “raw” data-based model, however,

correctly reflects the discrete multi-modal nature of the MPN probability distribution by including only values which, given the design of the testing procedure, are feasible. As a result, the “raw” data-based model prediction sets represent a more effective, defensible, and realistic approach to assessing model predictive performance.

To further clarify this point, we compare two approaches to calculating the predictive distribution of the MPN for a hypothetical “true” FIB concentration with a lognormal  $\text{LN}(c | \mu = \ln 300, \sigma = 0.16)$  probability distribution (Fig. 6). The first approach assumes that the MPN and FIB concentration ( $c$ ) are exchangeable and, therefore, have the same predictive distribution. This approach to calculating the MPN predictive distribution is consistent with the logic of equations (4) and (5), and is represented in Fig. 6 by a curved black line (MPN predictive distribution) and shaded grey area (MPN 95% prediction region). The second approach uses equations (6) and (7) to simulate the pattern of positive wells from an IDEXX Quanti-Tray<sup>®</sup>/2000 test, and then calculates (for each simulated pair of positive wells) an MPN value. The predictive distribution of the MPN based on the second approach is represented in Fig. 6 by vertical lines. All red vertical lines (regardless of height or location) represent the MPN 95% prediction set, defined as the set of *highest probability* MPN values for which the cumulative probability is at least 0.95 (Gronewold and Wolpert, 2008). Black vertical lines represent MPN values outside of the MPN 95% prediction set.

Fig. 6 suggests that the discrepancies between expected and observed model predictive performance in Fig. 5 may be caused

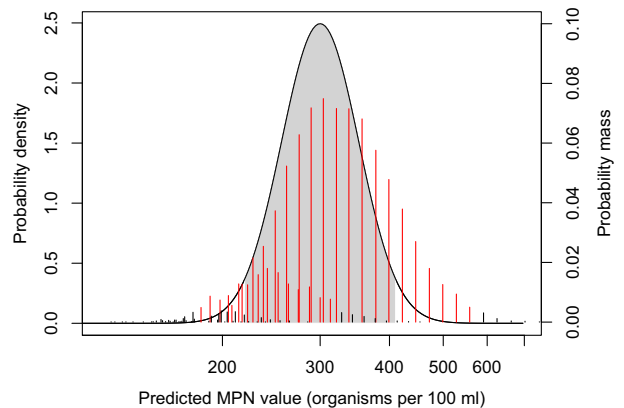


**Fig. 6 – Comparison between two approaches to calculating the predictive distribution of the MPN for a hypothetical FIB concentration  $c$  with a lognormal  $\text{LN}(c | \mu = \ln 300, \sigma = 0.16)$  probability distribution. The MPN predictive distribution and 95% prediction intervals associated with this FIB concentration based on the conventional MPN model are represented by the curved black line and the grey shaded area, respectively. The MPN distribution (for the same FIB concentration  $c$ ) derived from our “raw” data-based model is represented by vertical lines. All red vertical lines (regardless of height or location) represent the MPN 95% prediction set, defined as the set of *highest probability* MPN values for which the cumulative probability is at least 0.95 Gronewold and Wolpert (2008). Black vertical lines represent MPN values outside of the MPN 95% prediction set.**

by problems associated with using the MPN and the MPN-based model, a finding with significant implications for water quality assessments and management decisions. In particular, the relatively high number (and height, indicating probability mass) of vertical red lines in Fig. 6 which fall to the right or left of the shaded (grey) region indicates there is a significant chance for an MPN value to be both outside the prediction interval derived from the conventional MPN-based model and within the 95% prediction set of the proposed “raw” data-based model. Adjacent vertical red lines with very different heights reflect the multi-modal discrete nature of the MPN probability distribution. The vertical black lines in Fig. 6 within the shaded grey region indicate it is possible for an MPN value to be within the 95% prediction interval of the conventional MPN-based model yet not within the 95% prediction set derived from our proposed “raw” data-based model. These discrepancies are unacceptable to water quality managers making human health risk-based management decisions.

Aside from explicitly addressing these complications associated with modeling MPN values and providing a more realistic basis for assessing model predictive performance, our proposed “raw” data-based modeling approach explicitly distinguishes between intrinsic bias and variability introduced through a serial dilution analysis procedure (as discussed in Best and Rayner, 1985; Garthright, 1993, 1997), and variability in FIB fate and transport. These two sources of variability affect inactivation rate estimates and model forecasts in very different ways, yet they are not distinguishable in the conventional MPN-based model (equations (2) and (3)), potentially leading to overly conservative prediction intervals (see, for example, the relatively high calculated value of the residual error standard deviation for the EC MPN-based model in Fig. 3) and an inappropriate level of confidence in the estimate of the inactivation rate (as indicated by the variability in the width of ENT inactivation rate confidence intervals in Fig. 3).

Advantages of the proposed “raw” data-based model arise, in part, from an explicit acknowledgement that the pattern of positive wells from any serial dilution analysis experiment is a sufficient statistic (for definitions, see Bernardo and Smith, 1994, pp. 191–192) which can be expressed in a probabilistic framework through a binomial probabilistic distribution. In other words, the pattern of positive wells (along with the dilution factor, and volume of each well) contains all of the information necessary to quantify the likelihood function for the “true” FIB concentration  $c$ . In contrast, the MPN is not a complete summary of that information. We argue, therefore, that there is little relative benefit to the existing practice of calculating and reporting an MPN value when compared to the less common practice of reporting the pattern of positive wells (or tubes) alone. This approach, of course, would allow modelers and water resource managers alike to better understand the sources of uncertainty and variability in water quality measurements, and to more appropriately propagate them into model parameter estimates and model forecasts.

Finally, the “raw” data-based model could be improved by assuming that the dispersion of FIB cells in a sample aliquot is greater than that represented by equations (6) and (7), which are based on the assumption that the number of FIB cells in a sample has a Poisson  $Po(\lambda)$  probability distribution with mean and variance  $\lambda$ . Previous authors (El-Shaarawi et al., 1981; Christian and

Pipes, 1983, for example) have suggested that the dispersion of organisms in a sample aliquot may be more appropriately reflected by a negative binomial probability distribution. We leave exploration of the negative binomial model and its effect on inactivation rate assessments for future research, but suspect that it might improve model performance.

Ongoing and future opportunities for applying our modeling approach are found in a broad range of environmental and public health-related disciplines. For example (Harris et al. (1998), utilize MPN data in the analysis of planktonic diatom concentrations in sediment samples and cite similar studies using MPN calculations (e.g. Larrazabal et al., 1990; An et al., 1992). (Eckford and Fedorak (2005) use an MPN method to assess nitrate-reducing bacteria growth in oil fields, and (Fegan et al. (2004) present a series of studies enumerating *E. coli* 0157 in cattle feces using MPN procedures. Additional examples of MPN-based environmental assessment include soil and groundwater composition analysis (Menyah and Sato, 1996; Papen and von Berg, 1998) and aquifer contamination studies (Bekins et al., 1999). A specific example of an MPN-based assessment of fecal contamination in recreational water bodies is the Oregon Beach Monitoring Program (Neumann et al., 2006). This program, while acknowledging environmental conditions as potential sources of data variability, applies MPN point estimates of FIB concentration rather than probabilistic estimates, and therefore represents the type of study which could utilize, and potentially be improved by, our modeling strategy.

---

## 5. Conclusions

The following is a list of conclusions drawn from our study:

- FIB dark inactivation rates may vary with initial FIB concentration, but the relationship depends on FIB species, and the choice of a calibration model. We find, for example, that EC dark inactivation rates tend to decrease as initial EC concentrations decrease, but that ENT dark inactivation rates are relatively consistent across different ENT concentrations.
- We have demonstrated potential benefits of a new modeling strategy which uses the pattern of positive wells or tubes from a serial dilution FIB quantification experiment as “raw” data in a FIB water quality assessment. This approach helps propagate uncertainty in FIB concentration estimates into inactivation rates and model-based water quality forecasts while potentially simplifying the data recording process.
- Our proposed “raw” data-based model represents a more general class of Bayesian hierarchical and multi-level modeling strategies (for a detailed description, see Gelman and Hill, 2007) which provide an ideal structure for encoding the pattern of positive wells or tubes from a serial dilution analysis experiment as random variables. This model structure also allows us to infer inactivation rates (and other model parameters) by combining previously documented values with empirical evidence from our own study using Bayes’ theorem.
- We have demonstrated that our proposed “raw” data-based modeling approach performs as well as (if not better than) a conventional MPN-based model, yet avoids much of the burden of appropriately interpreting MPN values and their confidence limits.

- Laboratory-scale inactivation rate estimates are not necessarily transferable to more complex “real-world” mechanistic models. These estimates, instead, should be critically evaluated depending on the modeling context in which they were derived. Minor variations in how uncertainty is addressed, for example, can lead to very different parameter estimates for a given model, and can subsequently effect empirical relationships, model forecasts, and model-based management decisions.

United States Environmental Protection Agency, through its Office of Research and Development, partially funded and collaborated in the research described here. It has been subjected to Agency review and approved for publication. This paper is GLERL contribution number XX-XXXX. The authors thank Jim Wickham, Ibrahim Alameddine, James Christian, and two anonymous reviewers for their comments on the manuscript.

## Acknowledgements

This study was partially funded by the North Carolina Division of Water Quality (Contract No. EW05049). In addition, the

```

model{
  for(j in 1:J) {
    y1[j] ~ dbin(p1[j],n1)
    y2[j] ~ dbin(p2[j],n2)
    y3[j] ~ dbin(p1[j],n1)
    y4[j] ~ dbin(p2[j],n2)
    p1[j] <- 1-exp(-(c[j]/100)*v1/d)
    p2[j] <- 1-exp(-(c[j]/100)*v2/d)
    c[j] <- exp(log.c[j])
    log.c[j] ~ dnorm(mu[j],tau)
    mu[j] <- b[b.grp.bug[j]]-
      k[k.grp.bug[j]]*t[j]
  }

  d <- 10
  v1 <- 1.86
  v2 <- 0.186
  n1 <- 49
  n2 <- 48

  for (n in 1:18) {
    b[n] ~ dnorm(0, tau_b)
  }

  for (i in 1:6){
    k[i] ~ dt(0.15,1,3)
  }

  tau <- pow(sigma,-2)
  sigma ~ dunif(0,20)
  tau_b <- pow(sigma_b,-2)
  sigma_b ~ dunif(0,20)
}

```

## Appendix

The following code was used in WinBUGS to calibrate the proposed “raw” data-based (Bayesian) model:

```

# J = total number of samples = 72;
# No. pos. large wells - sample A;
# No. pos. small wells - sample A;
# No. pos. large wells - sample B;
# No. pos. small wells - sample B;
# Prob. of pos. large well;
# Prob. of pos. small well;
# EC or ENT conc. (org/100 ml);
# First-order loss model for log-
# concentration mean;
# t = time (days);
# ‘b.grp.bug’ and ‘k.grp.bug’
# indicate experiment--based groups
# of intercept and inactivation
# rates values (indexed by ‘n’ and
# ‘i’ below);

# Dilution factor;
# Large well volume (ml);
# Small well volume (ml);
# Total number large wells;
# Total number small wells;

# Number of experiments;
# Model intercept;

# Different experiment "types";
# Informative prior on k;

# Precision of model residuals;
# Standard dev. of model residuals;
# Precision of model intercept;
# Standard dev. of model intercept;

```

- An, K.H., Lassus, P., Maggi, P., Bardouil, M., Truquet, P., 1992. Dinoflagellate cyst changes and winter environmental-conditions in Vilaine Bay, Southern Brittany (France). *Botanica Marina* 35 (1), 61–67.
- Ashbolt, N.J., Grohmann, G.S., Kueh, C.S.W., 1993. Significance of specific bacterial pathogens in the assessment of polluted receiving waters of Sydney, Australia. *Water Science and Technology* 27 (3/4), 449–452.
- Auer, M.T., Niehaus, S.L., 1993. Modeling fecal coliform Bacteria—I. Field and laboratory Determination of loss Kinetics. *Water Research* 27 (4), 693–701.
- Bayes, T., 1763. An essay towards solving a problem in the doctrine of chances. *Philosophical Transactions of the Royal Society of London* 53, 370–418.
- Bekins, B.A., Godsy, E.M., Warren, E., 1999. Distribution of microbial physiologic types in an aquifer contaminated by crude oil. *Microbial Ecology* 37, 263.
- Benham, B.L., Baffaut, C., Zeckoski, R.W., Mankin, K.R., Pachepsky, Y.A., Sadeghi, A.M., Brannan, K.M., Soupier, M.L., Habersack, M.J., 2006. Modeling bacteria fate and transport in watersheds to support TMDLs. *Transactions of the ASABE* 49 (4), 987–1002.
- Bernardo, J.M., Smith, A.F.M., 1994. *Bayesian Theory*. John Wiley & Sons, Ltd., West Sussex, UK.
- Berry, D.A., 1996. *Statistics: A Bayesian Perspective*. Duxbury Press, Belmont, California.
- Best, D.J., Rayner, J.C.W., 1985. A comparison of the MPN and Fisher-Yates estimators for the density of organisms. *Biometrical Journal* 27 (2), 167–172.
- Boehm, A., Ashbolt, N., Colford, J., Dunbar, L., Fleming, L., Gold, M., Hansel, J., Hunter, P., Ichida, A., McGee, C., Soller, J.A., Weisberg, S.B., 2009. A sea change ahead for recreational water quality criteria. *Journal of Water and Health* 7 (1), 9–20.
- Bolstad, W.M., 2004. *Introduction to Bayesian Statistics*. Wiley-Interscience, Hoboken, NJ.
- Borsuk, M., Clemen, R., Maguire, L., Reckhow, K., 2001. Stakeholder values and scientific modeling in the Neuse River watershed. *Group Decision and Negotiation* 10 (4), 355–373.
- Borsuk, M., Stow, C., 2000. Bayesian parameter estimation in a mixed-order model of BOD decay. *Water Research* 34 (6), 1830–1836.
- Bowie, G., Mills, W., Porcella, D., Campbell, C., Chamberlin, C., 1985. *Rates, Constants, and Kinetics Formulations in Surface Water Quality Modeling*, second ed. United States Environmental Protection Agency Office of Research and Development Environmental Research Laboratory, Washington, D.C.
- Chambers, J.M., Hastie, T.J., 1991. *Statistical Models in S*. CRC Press, Inc., Boca Raton, FL, USA.
- Christian, R.R., Pipes, W.O., 1983. Frequency distributions of coliforms in water distribution systems. *Applied and Environmental Microbiology* 45 (2), 603–609.
- Eckford, R.E., Fedorak, P.M., 2005. Applying a most probable number method for enumerating planktonic, dissimilatory, ammonium-producing, nitrate-reducing bacteria in oil field waters. *Canadian Journal of Microbiology* 51 (8), 725–729.
- Efron, B., Tibshirani, R.J., 1993. *An Introduction to the Bootstrap*. Chapman & Hall/CRC.
- El-Shaarawi, A.H., Esterby, S.R., Dutka, B.J., 1981. Bacterial density in water determined by Poisson or negative binomial distributions. *Appl. Environ. Microbiol.* 41 (1), 107–116.
- Fegan, N., Higgs, G., Vanderlinde, P., Desmarchelier, P., 2004. Enumeration of *Escherichia coli* O157 in cattle faeces using most probable number technique and automated immunomagnetic separation. *Letters in Applied Microbiology* 38 (1), 56–59.
- Ferguson, C., Husman, A.M.D., Altavilla, N., Deere, D., Ashbolt, N., 2003. Fate and transport of surface water pathogens in watersheds. *Critical Reviews in Environmental Science and Technology* 33 (3), 299–361.
- Fischer, H.B., 1979. *Mixing in Inland and Coastal Waters*. Academic Press, New York.
- Food and Drug Administration and Interstate Shellfish Sanitation Conference, 2005. *National Shellfish Sanitation Program – guide for the control of molluscan shellfish*.
- Fries, J., Characklis, G., Noble, R., 2006. Attachment of fecal indicator bacteria to particles in the Neuse River Estuary, NC. *Journal of Environmental Engineering* 132, 1338.
- Fries, J., Characklis, G., Noble, R., 2008. Sediment–water exchange of *Vibrio* sp. and fecal indicator bacteria: implications for persistence and transport in the Neuse River Estuary, North Carolina, USA. *Water Research* 42 (4–5), 941–950.
- Garthright, W.E., 1993. Bias in the logarithm of microbial density estimates from serial dilutions. *Biometrical Journal* 35 (3), 299–314.
- Garthright, W.E., 1997. A Bayesian analysis of serial dilutions offers a worse positive bias than the MPN and proposes an inappropriate interval estimate. *Food Microbiology* 14 (5), 515–517.
- Gelman, A., Carlin, J.B., Stern, H.S., Rubin, D.B., 2004. *Bayesian data analysis*. Chapman & Hall/CRC. Florida, Boca Raton.
- Gelman, A., Hill, J., 2007. *Data Analysis Using Regression and Multilevel/Hierarchical Models*. Cambridge University Press, New York, NY.
- Ghinsberg, R.C., Dov, L.B., Sheinberg, Y., Nitzan, Y., Rogol, M., 1994. Monitoring of selected bacteria and fungi in sand and sea-water along the Tel-aviv coast. *Microbios* 77 (310), 29–40.
- Griffin, D., Lipp, E., McLaughlin, M., Rose, J., 2001. Marine recreation and public health microbiology: quest for the ideal indicator. *BioScience* 51 (10), 817–826.
- Gronewold, A.D., Borsuk, M.E., Wolpert, R.L., Reckhow, K.H., 2008. An assessment of fecal indicator bacteria-based water quality standards. *Environmental Science & Technology* 42 (13), 4676–4682.
- Gronewold, A.D., Qian, S.S., Wolpert, R.L., Reckhow, K.H., 2009. Calibrating and validating bacterial water quality models: a Bayesian approach. *Water Research* 42, 2688–2698.
- Gronewold, A.D., Wolpert, R.L., 2008. Modeling the relationship between most probable number (MPN) and colony-forming unit (CFU) estimates of fecal coliform concentration. *Water Research* 42 (13), 3327–3334.
- Harris, A.S.D., Jones, K.J., Lewis, J., 1998. An assessment of the accuracy and reproducibility of the most probable number (MPN) technique in estimating numbers of nutrient stressed diatoms in sediment samples. *Journal of Experimental Marine Biology and Ecology* 231 (1), 21–30.
- Huang, J.J., McBean, E.A., 2007. Using Bayesian statistics to estimate the coefficients of a two-component second-order chlorine bulk decay model for a water distribution system. *Water Research* 41 (2), 287–294.
- Hurley, M.A., Roscoe, M.E., 1983. Automated statistical analysis of microbial enumeration by dilution series. *Journal of Applied Bacteriology* 55 (1), 159–164.
- Ihaka, R., Gentleman, R., 1996. R: a language for data analysis and graphics. *Journal of Computational and Graphical Statistics* 5 (3), 299–314.
- Larrazabal, M.E., Lassus, P., Maggi, P., Bardouil, M., 1990. Modern dinoflagellate cysts in Vilaine Bay–Southern Britain (France). *Cryptogamie Algologie* 11 (3), 171–185.
- Lunn, D.J., Thomas, A., Best, N., Spiegelhalter, D., 2000. WinBUGS–A Bayesian modelling framework: concepts, structure, and extensibility. *Statistics and Computing* 10 (4), 325–337.

- McBride, G.B., 2003. Preparing exact most probable number (MPN) tables using occupancy theory, and accompanying measures of uncertainty. NIWA Technical Report 121, 62.
- Menyah, M.K., Sato, K., 1996. A proposal for re-evaluating the most probable number procedure for estimating numbers of *Bradyrhizobium* spp. *Biology and Fertility of Soils* 23 (2), 110–112.
- Mostaghimi, S., Brannan, K., Dillaha, T., 2002. Fecal coliform TMDL development: Case study and ramifications. *Water Resources Update* 122, 27–33.
- National Research Council, 2001. Assessing the TMDL approach to water quality management.
- Neumann, C.M., Harding, A.K., Sherman, J.M., 2006. Oregon Beach monitoring program: bacterial exceedances in marine and freshwater creeks/outfall samples, October 2002–April 2005. *Marine Pollution Bulletin* 52 (10), 1270–1277.
- Noble, R., Lee, I., Schiff, K., 2004. Inactivation of indicator microorganisms from various sources of faecal contamination in seawater and freshwater. *Journal of Applied Microbiology* 96 (3), 464–472.
- Noble, R.T., Moore, D.F., Leecaster, M.K., McGee, C.D., Weisberg, S.B., 2003a. Comparison of total coliform, fecal coliform, and enterococcus bacterial indicator response for ocean recreational water quality testing. *Water Research* 37 (7), 1637–1643.
- Noble, R.T., Weisberg, S.B., Leecaster, M.K., McGee, C.D., Ritter, K. J., Walker, K.O., Vainik, P.M., 2003b. Comparison of beach bacterial water quality indicator measurement methods. *Environmental Monitoring and Assessment* 81 (1), 301–312.
- Papen, H., von Berg, R., 1998. A most probable number method (MPN) for the estimation of cell numbers of heterotrophic nitrifying bacteria in soil. *Plant and Soil* 199 (1), 123–130.
- Press, S.J., 2003. *Subjective and Objective Bayesian Statistics: Principles, Models, and Applications*. Wiley-Interscience, Hoboken, NJ.
- Reckhow, K.H., Chapra, S.C., 1983. Confirmation of water quality models. *Ecological Modelling* 20 (2–3), 113–133.
- Sinton, L.W., Finlay, R.K., Lynch, P.A., 1999. Sunlight inactivation of fecal Bacteriophages and bacteria in sewage-polluted seawater. *Applied and Environmental Microbiology* 65 (8), 3605–3613.
- Thomann, R.V., Mueller, J.A., 1987. *Principles of Surface Water Quality Modeling and Control*. Harper & Row, New York.
- Weisberg, S., 2005. *Applied Linear Regression*, third ed.. In: *Wiley Series in Probability and Statistics* Wiley-Interscience, Hoboken, NJ.
- Woodward, R.L., 1957. How probable is the most probable number? *Journal of the American Water Works Association* 49 (1), 1060–1068.